



HAL
open science

Assessment of stratification and entrainment models in CATHARE 3 code against TPTF-H and Mantilla experiments

Sofia Carnevali, Philippe Fillion

► **To cite this version:**

Sofia Carnevali, Philippe Fillion. Assessment of stratification and entrainment models in CATHARE 3 code against TPTF-H and Mantilla experiments. NURETH-19 - The 19th International Topical Meeting on Nuclear Reactor Thermal Hydraulics, Mar 2022, Bruxelles (Conference virtuelle), Belgium. cea-03985842

HAL Id: cea-03985842

<https://cea.hal.science/cea-03985842v1>

Submitted on 13 Feb 2023

HAL is a multi-disciplinary open access archive for the deposit and dissemination of scientific research documents, whether they are published or not. The documents may come from teaching and research institutions in France or abroad, or from public or private research centers.

L'archive ouverte pluridisciplinaire **HAL**, est destinée au dépôt et à la diffusion de documents scientifiques de niveau recherche, publiés ou non, émanant des établissements d'enseignement et de recherche français ou étrangers, des laboratoires publics ou privés.

Copyright

ASSESSMENT OF STRATIFICATION AND ENTRAINMENT MODELS IN CATHARE 3 CODE AGAINST TPTF-H AND MANTILLA EXPERIMENTS

Sofia Carnevali and Philippe Fillion

Université Paris-Saclay, CEA,
Service de Thermo-hydraulique et de Mécanique des Fluides,
91191, Gif-sur-Yvette, France.
sofia.carnevali@cea.fr; philippe.fillion@cea.fr

ABSTRACT

This paper presents the assessment of CATHARE 3 code against tests performed in the horizontal TPTF (Two Phase Tests Facility) and Mantilla facilities. This activity falls within the framework of a benchmark conducted by the Forum & Network of System Thermal-Hydraulics Codes in Nuclear Reactor Thermal-Hydraulics (FONESYS). The aim of this benchmark is to highlight the capabilities of SYS-TH codes to predict the horizontal stratification criteria and the onset of droplet entrainment and entrainment rate. One of the objectives of TPTF experiments, conducted by JAERI (Japan), was to analyse the thermal-hydraulic responses in the horizontal legs of LWR. The considered tests were at steady state and saturated steam/water two-phase flow conditions for a pressure varying between 3 MPa and 12 MPa. CATHARE code simulations show a general rather good agreement with TPTF-H experimental results although some improvements like the stratification regime prediction seem necessary. In two horizontal test sections with different diameters, Mantilla carried out air/water experiments at low pressure, from stratified to annular flow conditions, including droplet entrainment. Entrainment fraction obtained both with the two-fluid 6-equation model and the 3-field model of CATHARE are compared against the experimental data. Some improvements of the existing models are proposed for the entrainment and deposition processes to better fit the experiment.

KEYWORDS

Horizontal flow, Stratified flow, Droplet entrainment, CATHARE

1. INTRODUCTION

One of the most important phenomena taking place in a Pressurized Water Reactor (PWR) during loss of coolant accident (LOCA) is the occurrence of the stratification in the horizontal parts of the primary circuit. Prediction of the flow regime becomes so crucial. The interfacial friction plays a significant role influencing the relative velocity, the void fraction calculation and so the stratification occurrence. In addition, when the gas velocity increases, droplet entrainment process can occur, affecting the flow behavior. In 2019, the FONESYS members (Forum & Network of System Thermal-Hydraulics Codes in Nuclear Reactor Thermal-Hydraulics), proposed an activity focused on the comparison of SYS-TH codes models aimed to investigate the horizontal stratification criteria and the onset of droplet entrainment [1], and a follow-up benchmark over TPTF horizontal [2] and Mantilla [3] experiments, allowing to analyze and compare code closure laws. CEA participated using CATHARE 3 V2.1 code [4], a multi-fluid thermal-hydraulic system code capable among all of simulating thermal phenomena occurring in the primary and secondary circuits of PWRs.

Two main transitions between the flow regimes are explicitly taken into account in the closure laws of the CATHARE two-fluid model: the transition between the stratified and non-stratified flow regimes, and the transition from annular to dispersed-annular flow regime [5]. De Crecy [6] laid the foundations for the future stratification model in CATHARE code focusing on the de-stratification criterion, and a detailed description of the whole stratification model implemented in CATHARE code was given by Bestion and Serre [7]. The authors presented validation results against the Moby Dick and METERO-H tests by which the intermittent-bubbly regime transition regime was observed. For flow conditions where both droplets and liquid film are present, the two-fluid model of CATHARE uses a correlation for onset of entrainment and for the entrainment fraction, i.e. the ratio of the droplet flowrate to the total liquid flowrate, both derived from the Steen-Wallis model [8]. A 3-field model, originally dedicated to study droplet entrainment in the core, has also been developed as option in CATHARE-3 and extended to the hot legs. Specific separate effect tests were devoted to droplet entrainment in horizontal pipes, and new models for the entrainment and deposition processes have been developed and validated against experiments in mist-stratified and mist-annular regimes [9].

This paper presents results of CATHARE simulation of experiments carried out in the TPTF-H and Mantilla horizontal test sections focusing on the stratification criterion and entrainment models implemented in CATHARE code. Paragraph 2 rapidly presents TPTF-H and Mantilla experiments. Stratification criterion and interfacial friction model implemented in CATHARE code and simulation results of TPTF-H facility are discussed in paragraph 3. Onset of entrainment and entrainment rate models are presented in paragraph 4. Conclusions and possible future improvements are found in paragraph 5.

2. TPTF-H AND MANTILLA FACILITIES

2.1. TPTF-H

In the 80's the Japan Atomic Energy Research Institute (JAERI) started an important research program, the so-called Ring of Safety Assessment Number 4 (ROSA-IV) [10]. It concerned an integral tests facility (LSTF), a separate effects tests facility, the Two Phase Test Facility (TPTF) and a code development strategy. Two test sections were proposed: the first one, vertical, aimed to better understand the holdup distribution in a core rod bundle and the second one, horizontal, focused on the comprehension of the flow regime transition, interphase heat transfer and the interfacial friction. This paper treats this latter configuration presented in Figure 1 predicting the stratified-wavy (SW) to slug (SL) transition and the stratified-wavy (SW) to wavy-dispersed (WD) transition in different high-pressure steam-water conditions (pressure varied between 30 and 120 bar) and different diameters. Indeed two test sections (TS) are proposed with the purpose to investigate the scale effects: the bigger section, 8-inch with a total length of 10 m and the smaller one, 4-inch and 6.4 m length. All tests are at saturated conditions and co-current flow.

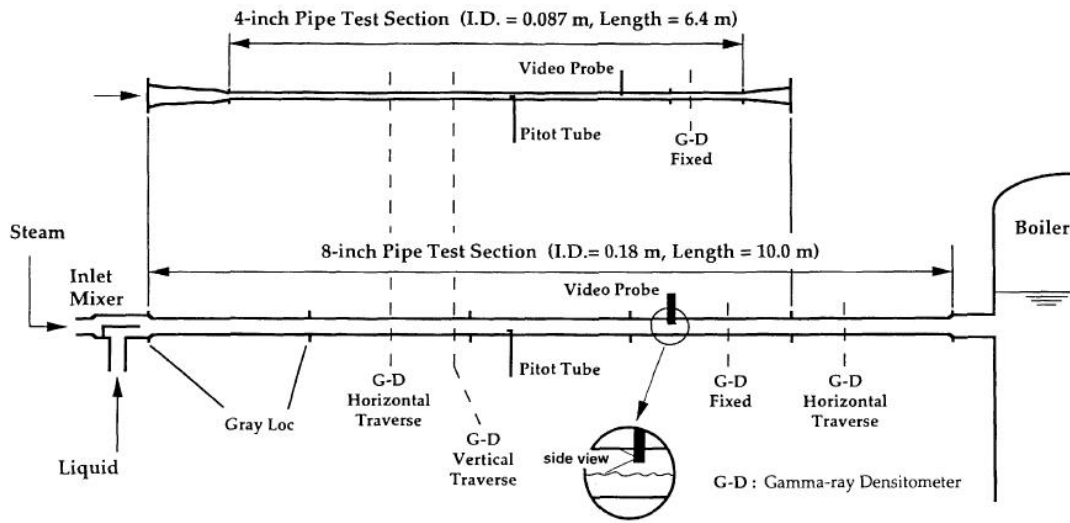


Figure 1. TPTF test section (from [10]).

Two different tee-shaped 12-inch mixers are fixed in the inlet of tests sections: the *bubbly* flow type, characterized by a bundle of horizontal perforated pipes that guarantee a well-mixed flow and the *separated* mixer, containing a horizontal plane by which a stratified flow is rapidly set up. Only tests performed with the separated flow mixer were assumed [10] to be representative of well-developed flow. A boiler is located at the outlet of the pipe where level corresponding to ± 0.5 m from the tests section axis.

A horizontally traversed γ -densitometers allows to measure void fractions at 17D (3.06 m from the entrance) and 48D (8.64 m from the entrance) for the 8-inch TS and 24D (2.088 m from the entrance) for the 4-inch TS. The maximum relative error was about 2% of the measured value. Flow regimes are determined by a visual observation and supported by measurements supplied by a vertically traversed and fixed 3-beams γ -densitometers and conductance probes. Transition to intermittent flow is confirmed also by a Pitot tube signal.

2.2. Mantilla

Mantilla [3] performed experiments in horizontal and inclined circular tubes with the objective to study the wave characteristics and the entrainment in the case of stratified, wavy-dispersed and dispersed annular flows. Two tests section were used: a horizontal 2-inch flow loop (inner diameter 0.0486 m) and a 6-inch flow loop (inner diameter 0.153 m) having a horizontal section and an inclinable section. Air-water, air-water-glycerin and air-water-butanol were carried out at low pressure (1-2.1 bar) and at 17-27°C fluid temperature, to study the influence of the fluid properties on the flow characteristics. In our study, only tests in air-water conditions in the horizontal test section are analyzed. Mantilla provides data on the onset of entrainment and the entrainment fraction for different liquid and gas superficial velocities. These data are collected far enough from the entrance of the test section to ensure a fully developed flow and in equilibrium conditions regarding the entrainment/deposition processes, suitable to validate or to develop model for the estimation of the entrainment fraction. Liquid film extractor technique was used to determine the entrainment fraction, with a maximum uncertainty of 0.065 for the 2-inch tests and 0.023 for the 6-inch tests. Onset of entrainment is visually determined by an internal borescope camera. Superficial gas velocity being increased by stepwise until an amount of droplets occur and hit the upper

part of the pipe. Experimental pressure drops close to the film measurement are also available, permitted to assess the interfacial friction and wall friction models.

3. ASSESSMENT OF STRATIFICATION IN CATHARE CODE

3.1. Stratification Criterion and Interfacial Friction Model

The current stratification criterion in CATHARE code [5,11] is the results of two contributions: the stratification stability which identifies the de-stratification limit based on the Kelvin-Helmholtz instability and the possible bubbly flow stability with the corresponding specific flow regime (slug, bubbly...). Since TPTF experiments permit to analyse the SW-SL transition, the following analysis exclusively focuses on the de-stratification criterion and the Kelvin-Helmholtz process.

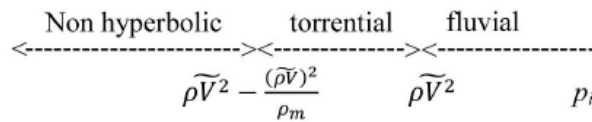
Two different linear stability analyses have been proposed: the high linear frequency stability and the marginal stability analysis. Both consist in identifying conditions where the growth of the void fraction rate is positive. The high frequency analysis takes into account only differential terms of the equation, neglecting viscous terms. It practically corresponds to the hyperbolicity limit of the system equations. De Crecy [6] shows that the characteristic equation from mass and momentum equation may be written as

$$\lambda^2 \rho - 2\lambda \tilde{\rho} \tilde{V} + \rho \tilde{V}^2 - p_i = 0 \quad (1)$$

with p_i is the pressure at the interface. The hyperbolicity condition is so defined as

$$p_i > \rho \tilde{V}^2 - \frac{(\tilde{\rho} \tilde{V})^2}{\tilde{\rho}_m} = \frac{\alpha(1-\alpha)\rho_l \rho_g (V_g - V_l)^2}{\tilde{\rho}_m} \quad (2)$$

where $\rho \tilde{V}^2 = \alpha \rho_l V_l^2 + (1-\alpha)\rho_g V_g^2$ and $\tilde{\rho}_m = \rho_l \alpha + \rho_g (1-\alpha)$ is the average fluid density weighted by the void fraction α , ρ_l and ρ_g are the liquid and gas densities, and V_l and V_g the liquid and gas velocities. Moreover one can demonstrate that for $p_i = \rho \tilde{V}^2$ the characteristic velocities of the system are the same and flow passes from torrential (supercritical to respect to the void waves) to fluvial (subcritical to respect to the void waves) as shown hereafter



Now this hyperbolicity limit correspond to a modified Froude number equal to

$$Fr = \frac{\rho_l \rho_g}{\tilde{\rho}_m (\rho_l - \rho_g) g D} (V_g - V_l)^2 + Fr_{\text{corr}} = 1 \quad (3)$$

where D is the pipe diameter. As in [12], a numerical factor Fr_{corr} corresponding to $10^{-2} / \alpha (1-\alpha)$ is added for numerical conditioning, preventing stratification at low or high void fraction.

On the other side, the marginal stability considers all terms of the equation and determines when at least one wavelength becomes unstable. In this case the numerical solution of the system is too complex for the code and it is simplified by $Fr = 1/4$ [5].

In other words, if $Fr < \frac{1}{4}$, flow is supposed stratified with an approximation of the marginal limit, if $Fr > 1$, solution does not exist (hyperbolic limit) and flow is practically unstable for all waves and, if Fr is into this range, an intermittent/slug flow is supposed. In parallel with the stratification criterion, the interfacial drag plays a crucial role to predict the regime flow.

The interfacial friction implemented in CATHARE code is validated over ECTHOR U-tube (loop-seals) and MHYRESA (Hot Leg) wavy data at low pressure and air-water conditions tests [12]. Expression of the interfacial coefficient in stratified flow regime has been derived from these experiments and depends on the void fraction, velocity, Froude number and hydraulic diameter.

3.2. TPTF-H CATHARE Nodalization and Benchmark Conditions

TPTF tests are simulated with CATHARE 3 V2.1 code. Figure 2 shows both the horizontal TS and the boiler volume for the 8-inch TS. Boiler, represented by a 0D volume, is modeled to be able to investigate the impact of outlet condition and in particular the different experimental water levels. Test section is modeled by a horizontal 1D component. Since void fractions are taken at 17D and 48D, simulated initial condition are shifted at 17D. A reduced test section is so modeled in agreement with benchmark instructions.

Void fraction, temperature and velocities are imposed at inlet condition. Saturated conditions are fixed. Pressure is controlled by an outlet condition. Level in the boiler is maintained constant. For the horizontal test section, choice of about 500 one-dimensional meshes is just to allow a representation as close as possible to the real geometry and in particular to the exit region (with an expansion zone).

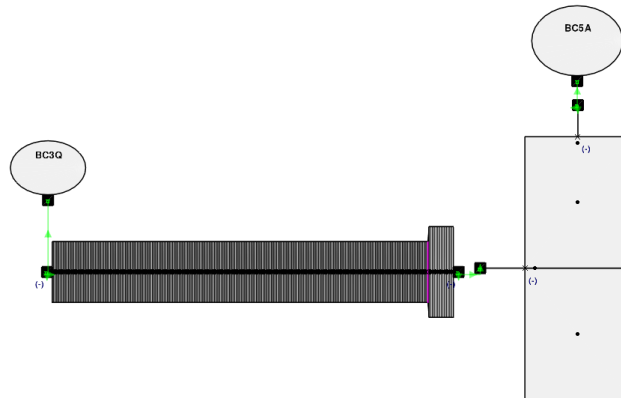


Figure 2. TPTF-H nodalization.

One-hundred-twenty-six co-current steady tests are chosen for the benchmark [1]:

- 6 tests in SW-SL transition performed with the 4-inch TS and the separated flow mixer. Tests are performed at 30 bar and the boiler liquid level is above the TS outlet nozzle.
- 56 tests in ST or SW are performed with the 8-inch TS and the bubbly flow mixer. Pressure varies between 75 bar and 120 bar. The boiler liquid level was either below or above the TS outlet nozzle. Tests were in fluvial or torrential flow conditions according to the Gardner and de Crecy criteria [6]. A more detailed analysis [1] showed that authors [2] inverted the liquid hold up $(1-\alpha)$ instead of the void fraction α for some of the tests at very low flow conditions. These experimental tests are so hereafter

corrected. The inlet mixer does not allow to obtain a well-developed flow and fluid does not reach the transition limit.

- 64 tests in SW, SL, WD, SW-SL and SW-WD transitions are obtained with the 8-inch TS and the separated flow mixer. Pressure is between 30 bar and 86 bar. The boiler liquid level was above the TS outlet nozzle (roughly 0.5 m above). Remember that these tests are representative of a full-developed flow thank to the inlet condition and transition to intermittent flow is observed. In addition, to better approximate a well-developed flow, practically all tests are in supercritical condition, except two. These tests are so not affected by outlet conditions (liquid level). A difference of <3% is observed between the 17D and 48D void fraction measurements; it is so assumed as constant all along the TS.

3.3. Analysis of TPTF-H calculated results

Figure 3 and Figure 4 show the comparison between the CATHARE stratification criterion (red line) and the experimental results for both 8-inch and 4-inch TS, in the (J_g, J_l) -plane, where $J_l = (1 - \alpha)V_l$ and $J_g = \alpha V_g$ are respectively the liquid and gas superficial velocities. Separated mixer experimental results are expressed with full markers, differently for bubbly mixer tests. High (H) and low (L) levels are represented. Results show that the code generally overpredicts the stratification limit expressed by black triangular markers (SW-SL). Moreover, at 75 bar, for high void fractions (high gas superficial velocity J_g and low liquid superficial velocity J_l) model too strongly prevents the stratification and underpredicts some stratified tests.

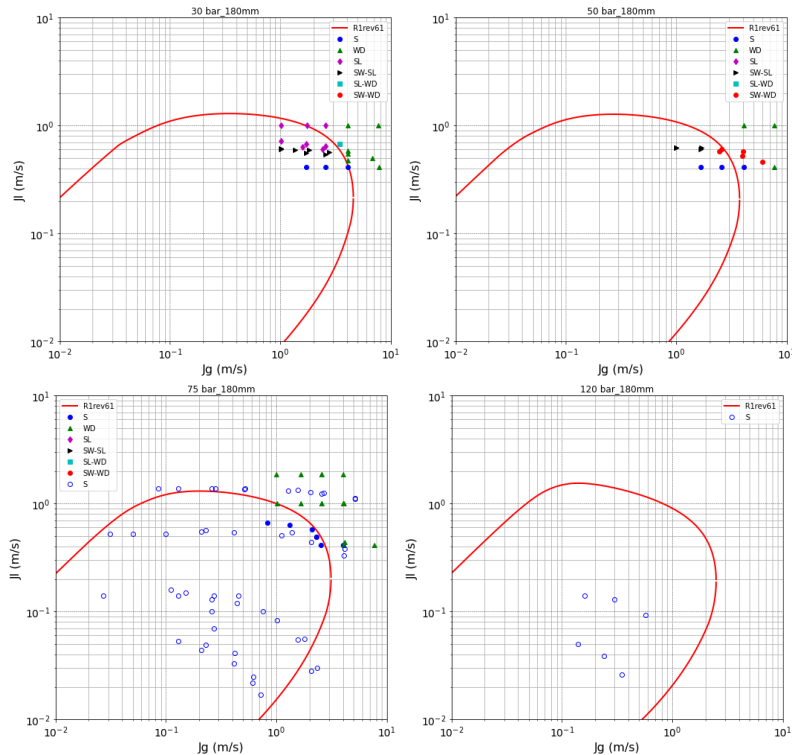


Figure 3. TPTF-H tests - Superficial velocities J_l and J_g for the 8-inch TS. Separated (full circles) and bubbly (void circles) mixers.

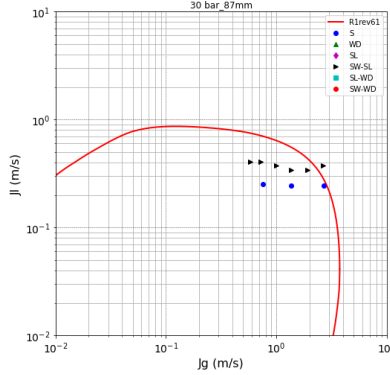


Figure 4. TPTF-H tests - Superficial velocities J_1 and J_g for the 4-inch TS.

Figure 5 shows the void fraction at 48D for the 8-inch TS with separated and bubbly mixers. Only calculated/experimental stratified tests are reported. Simulated void fraction is in good agreement within a difference to experimental results less than 10%. Despite that, a general overprediction of the void fraction is observed, probably due to a conservative character of the interfacial friction model.

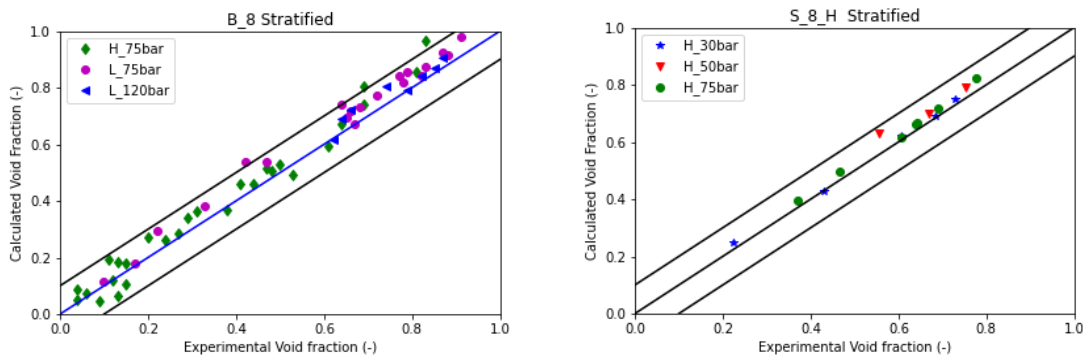


Figure 5. TPTF-H test - Calculated and Experimental void fraction for the 8-inch TS with B (bubbly) and S (separated) mixers.

Lastly Figure 6 presents void fractions calculated results along TS length. It is worth remembering that the void fraction for tests with separated mixer (S) does not practically change between the inlet and the exit condition. Figure 6 shows that CATHARE predicts well the void fraction distribution all along the TS length for torrential tests. Prediction of tests in the fluvial regime is more difficult since they are impacted by the outlet conditions and for these tests CATHARE shows some discrepancy. Despite the good prediction at 48D, an initial difference is observed. It is accentuated when flow is not well developed (*bubbly* mixer B) and the boiler level is high (H). A clear overprediction of the stratification limit and an over estimation of void fraction may be at the origin of this discrepancy. At date, further analyses are carried out to better investigate this point.

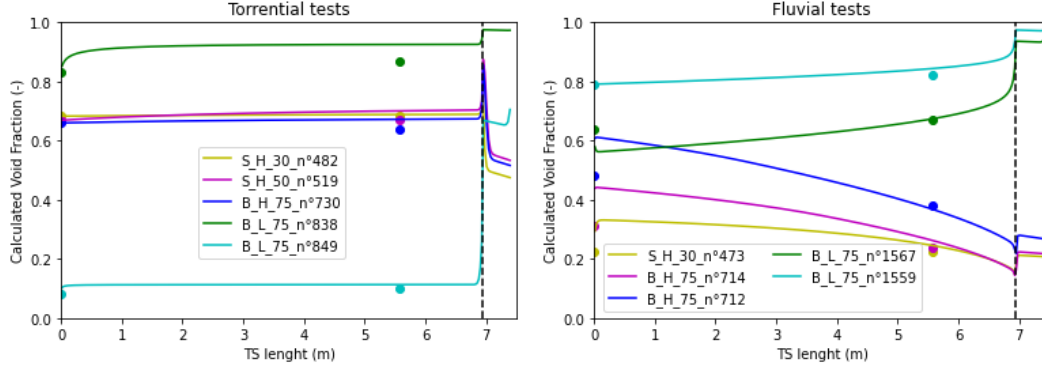


Figure 6. Calculated void fraction over TS length for the 8-inch TS. The dashed line represents the end of the TS. Starting from the left side, figures represent respectively torrential and fluvial tests. Single circle markers correspond to experimental results at 17D and 48D.

4. ASSESSMENT OF ENTRAINMENT MODELS IN CATHARE CODE

The entrainment fraction E (droplet flowrate over total liquid flowrate ratio) is estimated, for the 6-equation two-fluid model integrated in CATHARE 3, using a formulation derived from the Steen-Wallis [8] correlation

$$E = 1 - \min \left[1 - \left(\frac{J_{gcrit}}{J_g} \right)^2 \right] \quad (4)$$

The critical superficial gas velocity (J_{gcrit}) for the onset entrainment reads

$$J_{gcrit} = 2.1 \times 10^{-4} \frac{\sigma}{\mu_g} \sqrt{\frac{\rho_l}{\rho_g}} \quad (5)$$

where σ is the surface tension, μ_g the gas viscosity, ρ_l and ρ_g the liquid and gas densities respectively. CATHARE 3 code also includes a three-field model, based on an extension of the two-fluid model. Three sets of mass, momentum and energy conservation equations are solved for the three fields: the gas or vapor, the continuous liquid, and the dispersed liquid flowing in the form of entrained droplets. Models are present in CATHARE 3 for the simulation of the entrainment and deposition processes of the droplets within horizontal pipes, including both stratified and annular conditions for the liquid film [9]. These models have been developed and validated using air-water experiments at low pressure performed in large diameter horizontal pipes, including REGARD (pipe diameter 0.24 m) and Williams (pipe diameter 0.0953 m) databases. The model for the entrainment rate m_E is based on the Pan and Hanratty works [13]. The correlation reads

$$m_E = \frac{k'_A V_g^2 (\rho_g \rho_l)^{1/2}}{\sigma} \left(\frac{Q_l}{P_w} - \Gamma_{loE} \right) \quad (6)$$

where P_w is the perimeter of the pipe and Q_l the film flowrate.

The critical film flow Γ_{loE} corresponds to the liquid film flowrate per unit length at which the entrainment occurs. It is estimated by Pan and Hanratty from a correlation of the critical liquid Reynolds number

$$Re_{loE} = 7.3(\log_{10} w)^3 + 44.2(\log_{10} w)^2 - 263 \log_{10} w + 439 \quad (7)$$

where parameter $w = \mu_l/\mu_g\sqrt{(\rho_g/\rho_l)}$ depends on the liquid and gas viscosities μ_l and μ_g , and liquid and gas densities.

The dimensionless atomization constant $k'_A = 4.5 \times 10^{-7}$ used in the model implemented in CATHARE has been determined from REGARD and Williams data.

Deposition model, suggested by Neiss [14], takes into account two mechanisms acting on the droplet deposition in such conditions, namely turbulent diffusion and gravity:

$$m_D = kC = (k_{D,\text{grav}} + k_{D,\text{diff}})C \quad (8)$$

where C is the concentration of the droplets within the gas core and $k_{D,\text{grav}}$ and $k_{D,\text{diff}}$ are the deposition velocities relative to the gravity and relative to the turbulent diffusion, respectively.

For the gravity mechanism, the deposition constant

$$k_{D,\text{grav}} = g\tau_p \frac{S_{\text{grav}}}{S_{\text{tot}}} \quad (9)$$

is related to the terminal falling velocity of the droplet and the corresponding relaxation time τ_p , accounting the droplet diameter δ estimated using a specific correlation

$$\tau_p = \frac{1}{18} \frac{\delta^2 \rho_d}{\mu_g} \quad (10)$$

The diffusion turbulent part is modeled as

$$k_{D,\text{diff}} = 0.023 V_g Re_g^{-0.2} Sc_g^{-2/3} \frac{1}{1 + 2.5\alpha_d \frac{\rho_d}{\rho_g}} \quad (11)$$

where Re_g is the gas Reynolds number, Sc_g the Schmidt number, α_d the volumetric droplet fraction, and ρ_d the droplet density.

The final model for the deposition velocity k takes into account the stratification of the droplets in the lower part of the pipe, with an enhancement of the deposition process. The effective deposition velocity is thus

$$k_{D,\text{eff}} = f_D \cdot k_D \quad (12)$$

where $f_D = 4$.

4.1. Entrainment models against TPTF-H

The onset of entrainment model has been assessed against several TPTF-H tests at the transition SL-WD or ST-WD (see Figure 7). The modified Steen-Wallis model used by CATHARE underpredicts the critical gas velocity at which the liquid entrainment occurs. Original Steen-Wallis model, where 2.1×10^{-4} is replaced with 2.46×10^{-4} in equation (5), has been analyzed against these experiments by Nakamura et al. [15]. The authors attributed the poor results obtained by the model are due to the high liquid level (> 0.5 in the considered tests in our study) caused the gas velocity to be much larger than in the annular flows considered by Steen and Wallis for the development of their model. A criterion based on the gas Kutatelatze number, where the critical value $Ku = 3.2$ used as in the Crowe model [16] in rough turbulent regime, gives closer results but does not reproduce the experiments where the onset of

entrainment depends also on the liquid velocity or the liquid holdup. Several modifications of the Steen-Wallis model or a modified Kutateladze number, depending on the relative velocity between the vapour and liquid phases, have been also assessed by Nakamura et al. [15], allowing to better predict the onset of entrainment for the TPTF-H tests. However, the authors noticed that the proposed modified Steen-Wallis model does not take into account the dependence of the interfacial wave amplitudes on pressure observed in the experiment. Further analysis is still required to get a better reproduction of the onset of entrainment for these tests.

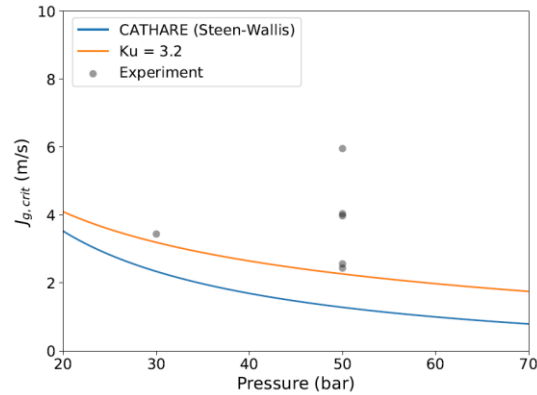


Figure 7. TPTF-H tests – Comparison of the onset of entrainment models against the experimental data.

4.2. Entrainment models against Mantilla

For the Mantilla tests, CATHARE model based on the Steen-Wallis correlation predicts too early the onset of entrainment for the runs performed in the 2-inch test section (see Figure 8). The model does not take into account the influence of the liquid velocity on the entrainment, and entrainment fraction tends to be overestimated at low liquid superficial velocity and underestimated when this parameter increases (Figure 9). For all tests on the 6-inch test section, the onset of entrainment is delayed by the CATHARE model (Figure 8), due the too high estimation of the critical gas velocity, and thus the models fails at predicting any entrainment (Figure 10). Regarding the stratification limit, most of the runs performed in the 2-inch test section are supposed to be in the non-stratified regime (transition to the annular of annular-mist regime) by CATHARE. Further analysis on the predicted regime can be found in the paper summarizing the benchmark results [17].

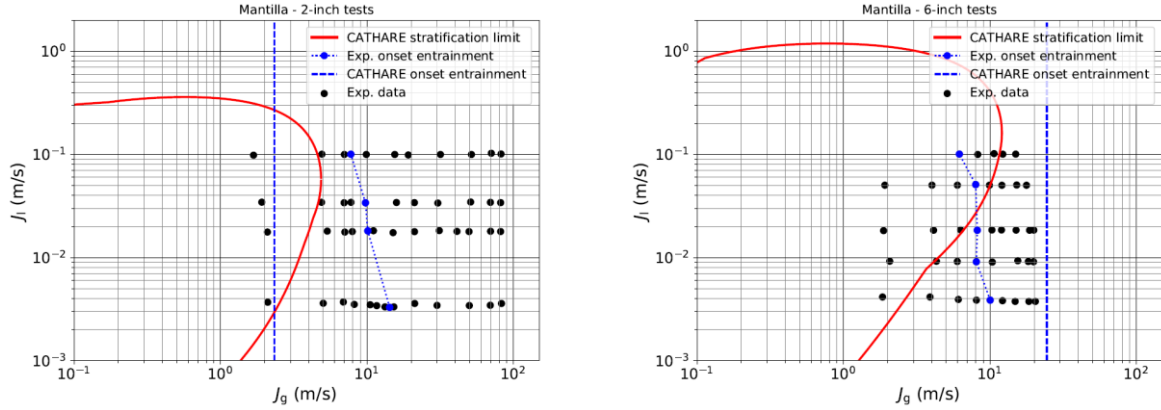


Figure 8. Mantilla tests – Comparison of the experimental and predicted onset of entrainment.

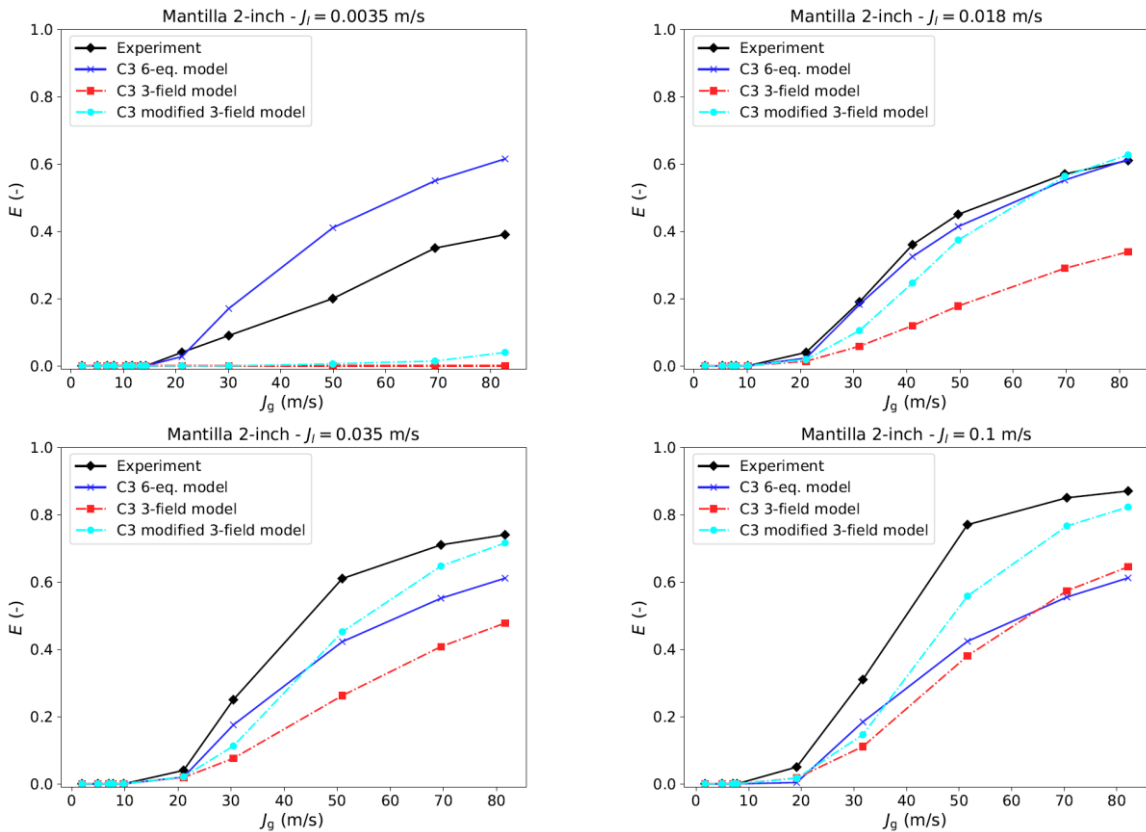


Figure 9. Mantilla 2-inch tests - Comparison of calculated entrainment fraction E by CATHARE 3 6-equation and 3-field models against experimental data.

Figure 9 and Figure 10 compare the entrainment fraction predicted by CATHARE 3 V2.1 code using the 6-equation model, based on the Steen-Wallis correlation and the entrainment fraction obtained using the three-field model against the experimental data. For the 2-inch cases at $J_1 = 0.0035$ m/s, the entrainment fraction obtained by the three-model is always null, because of the predicting liquid velocity

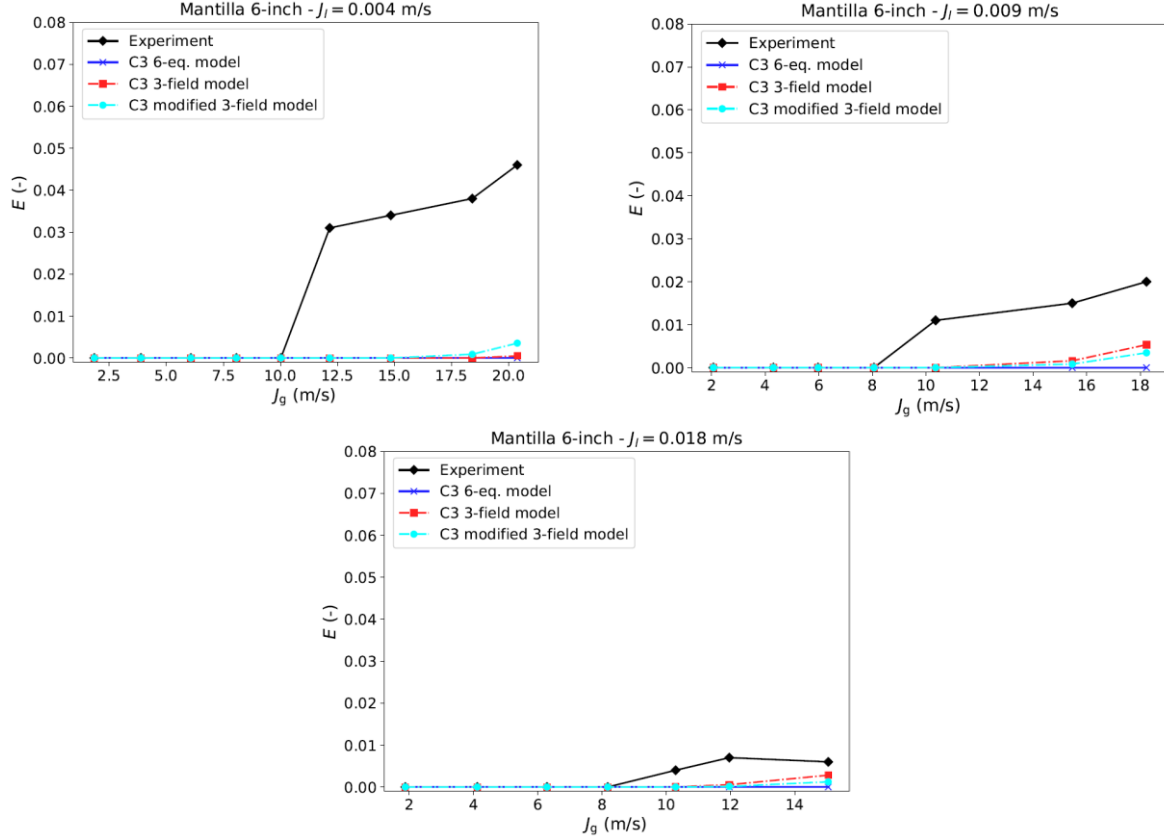


Figure 10. Mantilla 6-inch tests - Comparison of calculated entrainment fraction E by CATHARE 3 6-equation and 3-field models against experimental data.

at which the entrainment occurs, obtained by equation (7), is higher than the experimental conditions. In general, the three-field model tends to underpredict the entrainment fraction for the 2-inch tests. Same behavior is observed for the results obtained against the 6-inch tests. It is pointed out for these runs, the experimental entrainments diminish as the liquid superficial velocity increases, contrary to those obtained in the 2-inch test section. This behavior, well reproduced by the three-field model on Mantilla tests, was also observed by Vuong et al. [18] against other experiments at low-liquid-loading conditions, which are the case of 6-inch Mantilla tests.

In order to improve the results obtained by the current three-field model, several modifications of the correlations have been introduced for the present study. Predicted onset of entrainment is delayed using the current critical liquid number correlation with respect to the experiment. For a better fitting of the experimental data, we choose to set the critical liquid Reynolds number to 160, corresponding to those found by Ishii and Grolmes [19] for the occurrence of entrainment by the roll-wave shearing mechanism. Therefore, because critical liquid Reynolds number is a sub-model of the Pan-Hanratty correlation for the entrainment rate, atomization constant appearing in equation (6) to be reevaluated to $k'_A = 3.8 \times 10^{-7}$, from calibration against Mantilla, REGARD and Williams databases.

In the current deposition rate model, the gravity contribution can represent the major part of the deposition, the choice of a droplet size representative to the population of droplets in case of the deposition process, can be crucial for the predictions. In the current model, the mean Sauter diameter d_{32} , given by a correlation established from data obtained in horizontal pipes [9] has been selected. It is also used in the gas-droplet interfacial drag correlation in the 3-field model in CATHARE 3. Volume median

droplet diameter, also though as a representative size of the droplet, is used in several models (e.g. [20]). Introduction of the median volume droplet diameter d_{vm} in our deposition model have been thus assessed. From experimental data, it can be deduced from the mean Sauter diameter with the simple expression $d_{vm} = 1.67 d_{32}$. Finally, the expression of effective deposition velocity (see equation (12)) has been replaced by $k_{D,eff} = 3.1k_D$, from calibration of the model on the Mantilla, REGARD and Williams databases.

Entrainment fraction estimated by the modified CATHARE 3 3-field model, compared to the current CATHARE 3 V2.1 3-field model, and the experimental data are plotted in Figure 9 and Figure 10. For the 2-inch cases at $J_l=0.0035$ m/s, the entrainment fraction obtained with the modified 3-field model is now non null for the highest gas superficial velocities, but remains underpredicted. For the other 2-inch series, the prediction of entrainment fraction is significantly improved. Less conclusions on the 6-inch series can be drawn, where the current model and the modified model both underestimate the entrainment fraction.

5. CONCLUSIONS

The CATHARE 3 6-equation model has been assessed against steam-water TPTF tests in saturation conditions at high pressure (30 – 120 bar), performed in two horizontal tests sections (inner diameter $D=0.087$ m and $D=0.1799$ m), in order to validate the stratification criterion and the interfacial friction in stratified flow regime. Against these tests, the stratification model generally over predicts the stratification limit. Moreover at 75 bar, for high void fractions (high gas superficial velocity and low liquid superficial velocity), the model strongly cuts the stratification and under predicts some stratified tests. Experimental void fractions are well predicted by the code for torrential tests (supercritical conditions). Prediction of fluvial tests (subcritical conditions) is more difficult since they are impacted by the outlet conditions and CATHARE shows some difficulty to predict the experimental behavior.

On TPTF- tests, the onset of entrainment model included in CATHARE, based on Steen-Wallis model, tends to significantly anticipate the experiments flow conditions at which the entrainment occurs, depending both on the gas and liquid velocities. This onset of entrainment model or and the entrainment rate used in the 6-equation approach in CATHARE do not allow to predict the results observed in the air-water Mantilla experiments, performed in two different tests section ($D=0.0496$ m and $D=0.153$ m). The onset of entrainment tends to be delayed by the CATHARE model for these tests in low-pressure conditions. Current 3-field model of CATHARE 3, included a correlation based of the Pan-Hanratty model for the entrainment rate and a deposition model derived from Neiss, qualitatively reproduces the entrainment fraction, but underestimate this quantity. Modifications of the entrainment rate and deposition rate correlations of the 3-field model improve significantly the prediction of the Mantilla 2-inch test series. Further analysis is required for the 2-inch test series at the lowest liquid superficial velocity.

ACKNOWLEDGMENTS

This work has been carried out in the framework of the NEPTUNE project, funded by CEA, EDF, Framatome and IRSN.

REFERENCES

1. M. Lanfredini et al., “Stratification criteria of 8 system codes and direct confrontation to TPTF and Mantilla data”, *The 19th International Topical Meeting in Nuclear Thermal Hydraulics, Nureth-19, Brussels, Belgium, March 6-11, 2022* [to be issued].

2. M. Kawaji, A. Anoda, H. Nakamura and T. Tasaka: "Phase and Velocity Distributions and Holdup in High-Pressure Steam/Water Stratified Flow in a Large Diameter Horizontal Pipe," *International Journal of Multiphase Flow*, **13**(2), pp. 145-159 (1987).
3. I. Mantilla, Mechanistic modeling of liquid entrainment in gas in horizontal pipes. PhD thesis, University of Tulsa, USA (2008).
4. R. Pr ea et al., "CATHARE-3 V2.1: the new industrial version of the CATHARE code" *Proceedings of Advances in Thermal Hydraulics (ATH'20)*, pp. 730-742 (2020).
5. D Bestion, "The physical closure laws in CATHARE", *Nuclear Engineering and Design* **124**, pp. 229-245 (1990).
6. F. de Crecy, "Modeling of Stratified two-phase flow in pipes, pumps and other devices," *International Journal of Multiphase Flow*, **12**, pp. 307-323 (1986).
7. D. Bestion and G. Serre, "On the modelling of two-phase flow in horizontal legs of a PWR," *Nuclear Engineering and Technology*, **44**(8) (2012).
8. D. A. Steen and G. B. Wallis. The transition from annular to annular-mist co-current two-phase downflow. Technical Report NYO-3114-2, AEC (1964).
9. P. Fillion, "Development of the CATHARE 3 three-field model for simulations in large diameter horizontal pipes", NURETH-18, Portland, USA (2019).
10. H. Nakamura, "Slug Flow Transitions in Horizontal Gas/Liquid Two-Phase Flows (Dependence on Channel Height and System Pressure for Air/Water and Steam/Water Two-Phase Flows)," JAERI-Research 96-022 Report, Tokai-Mura, Japan, May 1996.
11. G. Serre et al., "On the stratification criterion in the CATHARE code", *The 14th International Topical Meeting on Nuclear Reactor Thermal Hydraulics, NURETH-14, Toronto, Canada, September 25-30, 2011*.
12. G. Geffraye et al., "Analysis of the MHYRESA hot leg entrainment tests", *ICONE-8106, Baltimore, MD USA, April 2-6, 2000*.
13. L. Pan and T.J. Hanratty, "Correlation of entrainment for annular flow in horizontal pipes," *International Journal of Multiphase Flows*, **28**, pp. 385–408 (2002).
14. C. Neiss, "Mod elisation et simulation de la dispersion turbulente et du d ep ot de gouttes dans un canal horizontal," PhD thesis, Universit e de Grenoble, France (2013) [in French].
15. H. Nakamura, Y. Kukita and K. Tasaka, "Flow Regime Transition to Wavy Dispersed Flow for High-Pressure Steam/Water Two-Phase Flow in Horizontal Pipe", *Journal of Nuclear Science and Technology*, **32**(7), pp. 641-652 (1995).
16. C.T. Crowe, "Multiphase Flow Handbook (Mechanical Engineering)". CRC Press, Taylor&Francis Group (2006).
17. M. Landrefini et al., "Droplet entrainment prediction in horizontal flow by SYS-TH codes - recent analyses made within the FONESYS network", *19th International Topical Meeting in Nuclear Thermal Hydraulics, Nureth-19, Brussels, Belgium, March 6-11, 2022* [to be issued].
18. D. H. Vuong, C. Sarica, E. Pereyra, A. Al-Sarkhi, "Liquid droplet entrainment in two-phase oil-gas low-liquid-loading flow in horizontal pipes at high pressure", *International Journal of Multiphase Flow* **99**, pp. 383-396 (2018).
19. M. Ishii, M.A. Grolmes. "Inception criteria for droplet entrainment in two-phase concurrent film flow", *AIChE J.* **21**, pp. 308-318 (1975).
20. J. K. Schimpf, K. D. Kim, J. Heo and B. J. Kim, "Development of droplet entrainment and deposition models for horizontal flow," *Nuclear Engineering and Design*, **50**, pp. 379–388 (2018).